

Preparation of New Series of Poly(amide-imide) Reinforced Layer Silicate Nanocomposite Containing *N*-Trimellitimide-*L*-Alanine

Khalil Faghihi,^{1*} Masoumeh Soleimani,¹ and Meisam Shabani²

¹ Polymer Research Laboratory, Department of Chemistry, Faculty of Science, Islamic Azad University, Arak Branch, Arak, Iran.

² Young Researchers Club, Arak Branch, Islamic Azad University, Arak, Iran.
k-faghihi@araku.ac.ir, Fax: 0098-861-2774031.

Received January 24, 2011; accepted June 6, 2011

Abstract. A new poly(amide-imide)-montmorillonite series were generated through solution intercalation technique. Cloisite® 20A was used as a modified montmorillonite for ample compatibility with the poly(amide-imide) (PAI) matrix. The PAI **5** chains were synthesized by the direct polycondensation reaction of *N*-trimellitylimido-*L*-alanine (**3**) with 4,4'-diamino diphenyl ether (**4**) in the presence of triphenyl phosphite (TPP), CaCl₂, pyridine and *N*-methyl-2-pyrrolidone (NMP). Morphology and structure of the resulting PAI-nanocomposite films **5a-5d** with (5-20 Wt%) silicate particles were characterized by FTIR spectroscopy, X-ray diffraction (XRD), and scanning electron microscopy (SEM). The effect of clay dispersion and the interaction between clay and polymeric chains on the properties of nanocomposites films were investigated by using UV-Vis spectroscopy, thermogravimetric analysis (TGA), and water uptake measurements.

Key words: Poly(amide-imide), nanocomposite, solution intercalation technique, Polycondensation.

Resumen. Se generó una nueva serie de montmorillonita poliamido-imidas a través de la técnica de intercalación en solución. Como montmorillonita se empleó Cloisite® 20A con gran compatibilidad con la matriz de poli(amido-imido) (PAI). Las cadenas de PAI **5** se sintetizaron por reacción de policondensación directa de la *N*-trimellitylimido-*L*-alanina (**3**) con éter 4,4'-diaminodifenílico (**4**) en presencia de trifenilfosfita (TPP), CaCl₂, piridina y *N*-metil-2-pirrolidona (NMP). La morfología y estructura de las películas de PAI-nanocomposita con partículas de silicato (5-20% peso), **5a-5d**, se caracterizaron por espectroscopia FTIR, difracción de rayos X (XRD) y microscopia electrónica de barrido (SEM). Se investigaron, mediante espectroscopia UV-Vis, análisis termogravimétrico (TGA) y mediciones de absorción de agua, tanto el efecto de la dispersión de la arcilla como la interacción entre la arcilla y las cadenas poliméricas sobre las propiedades de las películas nanocompositas.

Palabras clave: Poliamido-imidas, nanocomposita, técnica de intercalación en solución, policondensación.

Introduction

Polymer-clay nanocomposites typically exhibited mechanical, thermal and gas barrier properties, which are superior to those of the corresponding pure polymers [1-9]. Unique properties of the nanocomposites are usually observed when the ultra fine silicate layers are homogeneously dispersed throughout the polymer matrix at nanoscale. The uniform dispersion of silicate layers is usually desirable for maximum reinforcement of the materials. Due to the incompatibility of hydrophilic layered silicates and hydrophobic polymer matrix, the individual nanolayers are not easily separated and dispersed in many polymers. For this purpose, silicate layers are usually modified with an intercalating agent to obtain organically modified clay prior to use in nanocomposite formation [10-11]. Also aromatic polyimides are well recognized as a class of high performance materials due to their remarkable thermal and oxidative stabilities and excellent electrical and mechanical properties for long time periods of operation [10-12]. Unfortunately, strong interaction between polyimide chains and their rigid structure make them intractable. Poor thermoplastic fluidity and solubility are the major problems for wide application of polyimides. Thus, to overcome these processing problems various approaches have been carried out by incorporating flexible units such as -NH-CO-, -O-, and -SO₂-, and some of which are commercialized [12-14]. Among them, polyamide-imide (PAI) is the most successful material, which combines the advantages of high-

temperature stability and processability [15-23]. In this article two PAI-nanocomposite films with 5, 10, 15 and 20% silicate particles containing chiral *N*-trimellitylimido-*L*-Alanine moiety in the main chain was prepared by using a convenient solution intercalation technique.

In this report, nanocomposites of poly(amide-imide) with organoclay have been synthesized using a solution technique. Poly(amide-imide) was prepared by reacting 4,4-diamino diphenyl ether (**4**) with *N*-trimellitylimido *L*-alanine (**3**) in *N*-methyl-2-pyrrolidone (NMP). Structure and morphology of the PAI-NC were determined by FT-IR, UV-Vis, XRD and SEM, TGA and water absorption measurements.

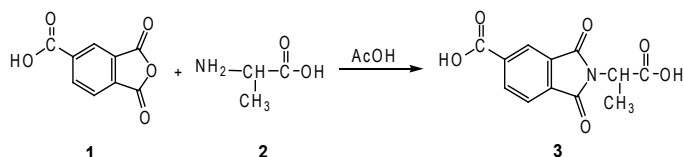
Results and Discussion

Monomer Synthesis

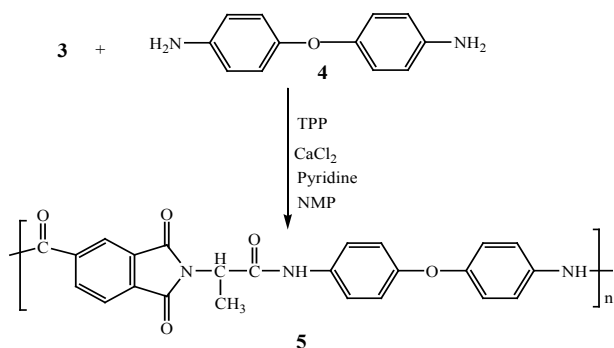
N-Trimellitylimido-*L*-alanine (**3**) was synthesized by the condensation reaction of one equimolar of trimellitic anhydride (**1**) with one equimolar of *L*-alanine (**2**) in an acetic acid solution (Scheme 1). The chemical structure of diacid **3** was confirmed by FT-IR and ¹H-NMR spectroscopy.

Polymer synthesis

Poly(amide-imide) **5** was synthesized by the direct solution polycondensation reaction of an equimolar mixture of diacid **3**,



Scheme 1. Synthetic route of *N*-trimellitylimido-*L*-alanine **3**.



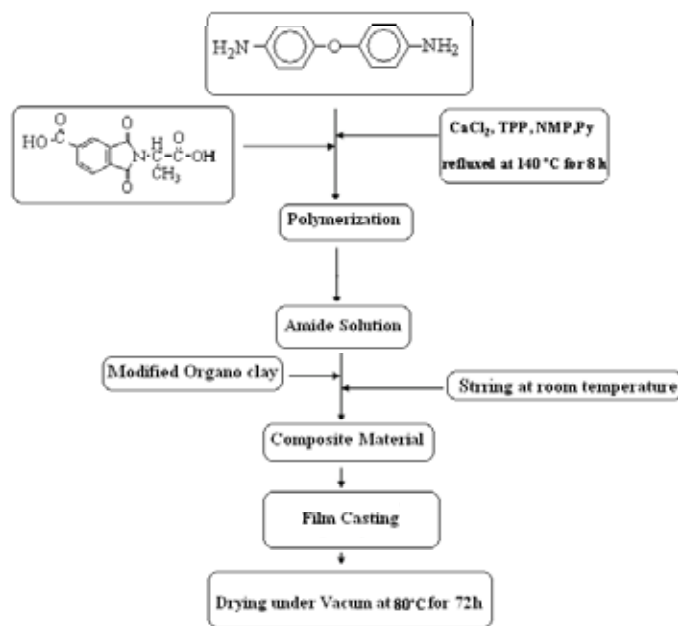
Scheme 2. Synthetic route of PAI **5**.

an equimolar mixture of diamine **4** by using triphenyl phosphite (TPP) and pyridine as condensing agents (Scheme 2). PAI **5** was obtained with good yield (97%) and good inherent viscosity at 25 °C in *N*-methyl-2-pyrrolidone (NMP) (0.64 dLg⁻¹). The structure of resulting polymer **5** was confirmed as PAI by using FTIR spectroscopy and elemental analyses. The resulting polymer have absorption band between 1780 and 1710 cm⁻¹ due to imide and amide carbonyl groups. Absorption bands around 1380 cm⁻¹ and 727 cm⁻¹ demonstrated the presence of the imide heterocyclic absorption in these polymers. Also absorption band of amide group appeared at 3414 cm⁻¹ (N-H stretching). The elemental analysis value of the resulting polymer was in good agreement with the calculated values for the proposed structure.

PAI-nanocomposite films

PAI-Nanocomposites were prepared by solution mixing of the appropriate amounts of Cloisite® 20A and PAI into 50 mL flask for a particular concentration. The mixture was agitated at a high speed for 24 h for uniform dispersion of organoclay in the PAI matrix. Different compositions of the hybrid materials having 5, 10, 15, and 20 wt.% organoclay were prepared as mentioned above to give nanocomposite films **5a-d**, respectively. Thin nanocomposite films were cast by pouring the hybrid solution into Petri dishes placed on a leveled surface. The solvent was evaporated at 70 °C for 8 h and hybrid films were further dried at 80 °C under vacuum to a constant weight.

PAI-nanocomposite films were transparent and yellowish brown in color. The incorporation of organoclay changed the color of films to dark yellowish brown. Moreover, a decrease in the transparency was observed at higher clay contents. Scheme



Scheme 3. Flow sheet diagram for the synthesis of PAI-nanocomposite films **5a-5d**.

3 show the flowsheet diagram and synthetic scheme for PAI-nanocomposite films **5a-5d**.

FT-IR spectroscopy analyses

FT-IR spectroscopy spectra of PAI-nanocomposite films **5b** and **5d** showed the characteristic absorption bands of the Al-O and Mg-O moieties at 1038, 510 and 458 cm⁻¹ respectively. The incorporation of organic groups in PAI-nanocomposite films was confirmed by the presence of peaks around 1772, 1720, 1383, 727 (imide rings) and 1660 (amide carbonyl group) cm⁻¹.

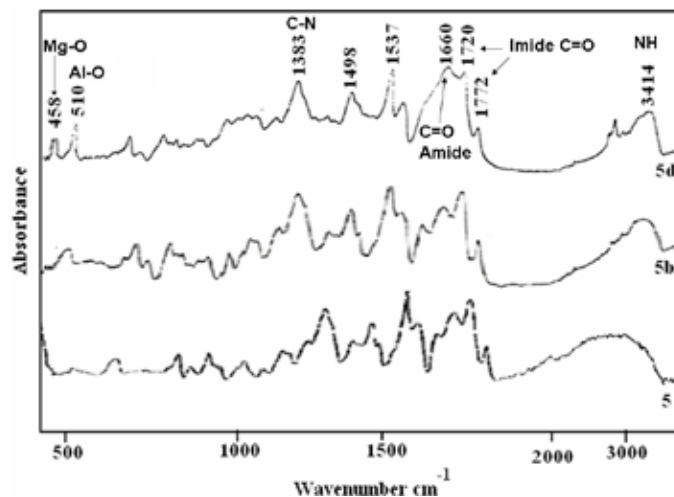


Figure 1. The FTIR spectra of PAI (**5**), **5b**, **5d**.

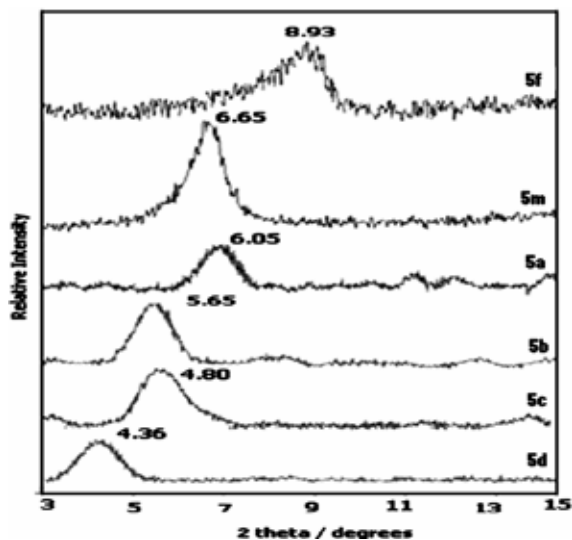


Figure 2. X-ray diffraction patterns of Cloisite® Na⁺ (**5f**), Organoclay (**5m**), PAI-nanocomposite films **5a**, **5b**, **5c**, and **5d**.

X-ray diffraction analysis

The XRD is most useful for the measurement of interlayer spacing of the organoclay upon the formation of the nanocomposites. It supplies information on the change of d-spacing of ordered immiscible and ordered intercalated nanocomposites. Fig. 3 shows the XRD patterns of PAI-nanocomposite films **5a-5d** containing 5-20 wt.% of silicate particles (Table 1). The Cloisite® Na gives a distinct peak around 2θ equal to 8.93, which corresponds to a basal spacing of around 1.00 nm. The organically modified (Cloisite® 20A) employed for the preparation of nanocomposites has a typical peak at 2θ equal to 6.65 (1.491 nm) increased d-spacing. When the amount of organoclay increased (5-20 wt.%) in the nanocomposites, small peaks appeared at $2\theta = 6.05, 5.65, 4.80$ and 4.36 corresponding to d-spacing 1.653, 1.623, 1.594 and 1.588 nm, respectively. These results indicated significant expansion of the silicate layer after insertion PAI chains. The shift in the diffraction peaks PAI-nanocomposite films confirms that intercalation has been taken place. This is direct evidence that PAI-nanocomposites have been formed as the nature of intercalating agent also affects the

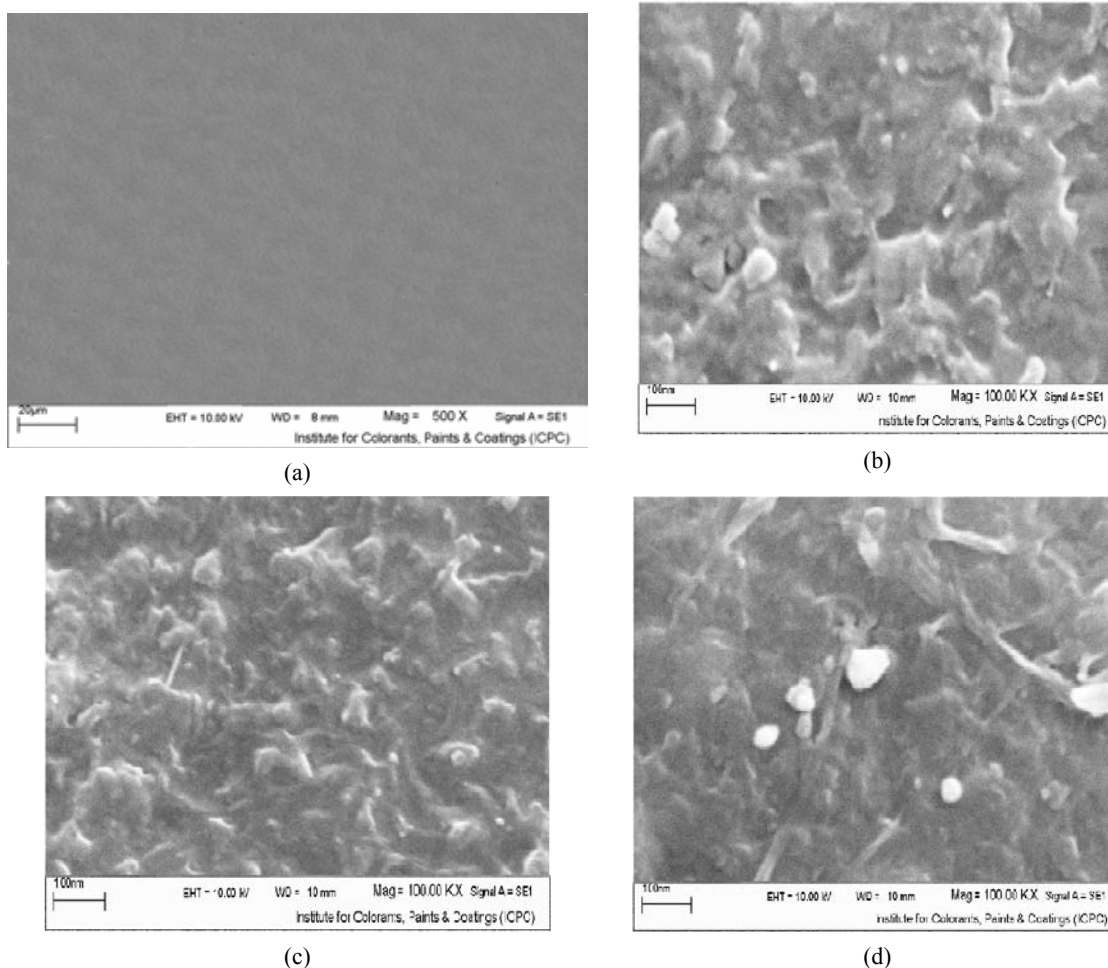


Figure 3. SEM micrographs of the PAI **5** (**a**) and nanocomposites with various silica contents (Wt%): (**b**) **5**; (**c**) **10**; (**d**) **15**.

organoclay dispersion in the polymer matrix. Usually there are two types of nanocomposites depending upon the dispersion of clay particles. The first type is an intercalated polymer clay nanocomposite, which consists of well ordered multi layers of polymer chain and silicate layers a few nanometers thick. The second type is an exfoliated polymer-clay nanocomposite, in which there is a loss of ordered structures due to the extensive penetration of polymer chain into the layer silicate. Such part would not produce distinct peaks in the XRD pattern [24]. In our PAI- nanocomposite films there are coherent XRD signal at 6.05°, 5.65, 4.80, and 4.36° related to 5, 10, 15, and 20 wt.% nanocomposite films, **5a-5d**, respectively.

Scanning electron microscopy

In order to investigate the morphology, fractured surfaces of PAI-nanocomposite films were studied using SEM. The micrographs of the PAI **5** (a) and nanocomposites containing 5, 10 and 15 wt% silica in the matrix are shown in Fig 3. The SEM images show the distribution of the silica with average size particles ranging from 20 to 39 nm. These results show a fine dispersion of silica particles in the matrix and when the concentration of inorganic phase is increased. Nanocomposite films have a very homogeneous distribution with no preferential accumulation of silica in any region across the films. The micrographs also indicate the presence of interconnected silica domains in the continuous polyamide phase, which demonstrates better compatibility between smaller silica nanoparticles and the PAI in the nanocomposite films.

Optical clarity of PAI-nanocomposite films

Optical clarity of PAI-nanocomposite films containing 5-20 wt.% clay platelets and neat PAI was compared by UV-Vis spectroscopy in the region of 260-800 nm. Fig. 5 show the UV-Vis transmission spectra of pure PAI and PAI-nanocomposite films containing 5-20 wt.% clay platelets. These spectra show that the UV-Visible region (250-800 nm) is affected by the presence of the clay particles and exhibiting low transparency reflected to the primarily intercalated composites. Results

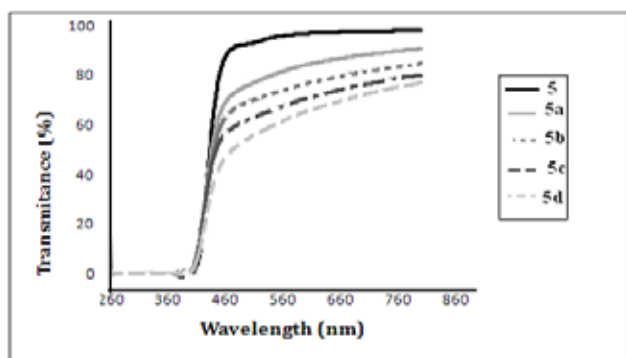


Figure 4. UV-Vis spectra of PAI **5**, PAI-nanocomposite films **5a-5d**.

Table 1. Transmittance data for PAI **5**, PAI-nanocomposite films **5a-5d**.

Sample	Cloisite® 20A (wt%)	Transmittance (%)				
		450 nm	500 nm	600 nm	700 nm	800 nm
5	0	81.52	92.65	96.88	97.59	98.10
5a	5	64.12	76.04	84.23	88.09	90.63
5b	10	53.62	69.25	76.51	81.21	84.63
5c	15	53.20	62.13	70.55	76.09	80.03
5d	20	43.01	54.54	65.39	72.10	76.85

shows that pure PAI and PAI-nanocomposite films various amounts of silica are transparent, and the transmittances recorded at 450, 500, 600, 700 and 800 nm for PAI and PAI-nanocomposite thickness were 81.52, 92.65, 96.88, 97.59 and 98.10 %, respectively Table 1. The maximum transmittance was found for the PAI (Table 1). The transparency of these nanocomposites depends upon the size and spatial distribution of silica particles in the PAI matrix. Nanocomposite films were transparent because the average size of the ceramic particles is smaller than the wavelength of light, and the distribution of particles is relatively uniform. Ultimately the tendency for the agglomeration of small particles into larger ones may increase, which decreases the homogeneity of the system. As particle size becomes larger, the transmittance values decrease.

Thermal Properties

The thermal properties of PAI-nanocomposite films containing 10 and 20 wt% clay platelets and neat PAI were investigated by TGA in a nitrogen atmosphere at a heating rate of 10 K/min (Fig. 6).

Initial decomposition temperature, 5% and 10% weight loss temperatures (T_5 , T_{10}) and char yields are summarized in Table 2.

These samples exhibited good resistance to thermal decomposition. T_5 for neat PAI and PAI-nanocomposite films containing 10 and 20 Wt% clay platelets ranged at 210-350 °C

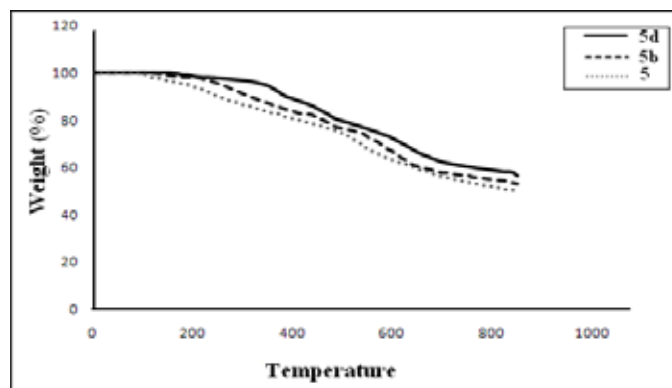


Figure 5. TGA curves of neat PAI **5** and PAI-nanocomposite films **5b** and **5d**.

Table 2. Thermal behaviors and Water uptake of neat PAI **5** and PAI-nanocomposite films **5b** and **5d**.

Polyimide	T ₅ (°C) ^a	T ₁₀ (°C) ^b	Char Yield ^c	Water uptake (%) ^d
5	210-220	260-270	49.65	16.25
5a	—	—	—	14.75
5b	260-270	300-310	52.82	12.5
5c	—	—	—	9.5
5d	340-350	385-395	56.22	1.2

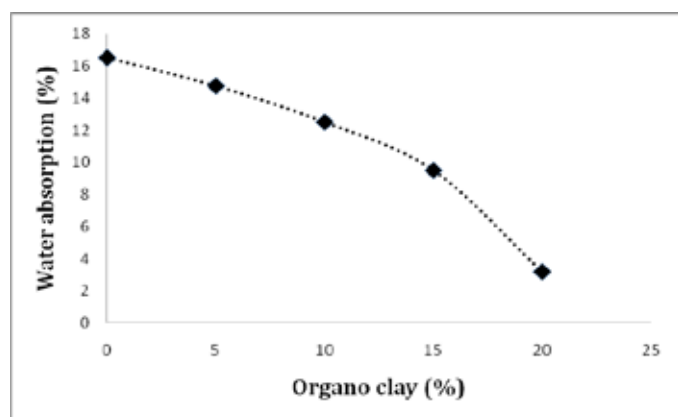
^{a,b} Temperature at which 5% or 10% weight loss was recorded TGA at a heating rate of 10 K/min in N₂.

^c Weight percentage of material left after TGA analysis at maximum temperature 800 °C in N₂.

and T₁₀ for them ranged from 260-395 °C, and residual weights at 800 °C ranged from 49.65 to 56.22% in nitrogen respectively. Incorporation of organoclay into the PAI matrix also enhanced the thermal stability of the nanocomposites. Thus, we can speculate that interacting PAIs chains between the clay layers serve to improve the thermal stability of nanocomposites. The addition of organoclay in polymeric matrix can significantly improve the thermal stability of PAI.

Water absorption measurements

The results showed maximum water uptake for the pure polyamide (16.25%) with monotonic but asymptotic decrease thereafter (Table 2). The exposure of polar groups to the surface of polymer where water molecules develop secondary bond forces with these groups. The clay platelets obviously restrict the access of water to the hydrogen-bonding sites on the polymer chains. The weight gain by the films gradually decreased as the clay content was increased. It is apparently due to the mutual interaction between the organic and inorganic phases. This interaction resulted in the lesser availability of polar groups to interact with water. Secondly, the impermeable clay layers mandate a tortuous pathway for a permeant to transverse the nanocomposite. The enhanced barrier characteristics, chemi-

**Figure 6.** Water absorption curves of PAI **5** and PAI-nanocomposite films **5a-5d**.

cal resistance and reduced solvent uptake PAI-nanocomposites all benefit from the hindered diffusion pathways through the nanocomposite [25].

Conclusions

The PAI-nanocomposites were successfully prepared using solution intercalation method. The structure and the uniform dispersion of organoclay throughout the PAI matrix were confirmed by FTIR, XRD and SEM analyses. The optical clarity and water absorption property of PAI-nanocomposites were decreased significantly with increasing the organoclay contents in PAI matrix. On the contrary the thermal stability of PAI-nanocomposites were increased significantly with increasing the organoclay contents in PAI matrix. The enhancements in the thermal stability of the nanocomposite films **5b** and **5d** caused by introducing organoclay may be due to the strong interactions between polymeric matrix and organoclay generating well intercalation and dispersion of clay platelets in the PAI matrix. Thermal and organosoluble properties can make these nanocomposites attractive for practical applications such as processable high-performance engineering plastics.

Experimental Section

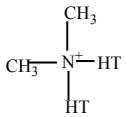
Materials

Trimellitic anhydride, *L*-Alanine, 4,4'-diamino diphenyl ether, acetic acid, triphenyl phosphite (TPP), CaCl₂, pyridine and *N*-methyl-2-pyrrolidone (NMP) were purchased from Merck Chemical Company and used without previous purification. Purified montmorillonite Cloisite[®] Na⁺ and the organocally modified Cloisite[®] 20A supplied by Southern Clay Products (TX), were used as polymer nanoreinforcement. The organic modifier and the interlayer distance of the clays are shown in Table 1 to account the structural modifications of the functionalizations.

Measurements

IR spectra were recorded on a Galaxy series FTIR 5000 spectrophotometer (England). Band intensities are assigned as weak (w), medium (m), strong (s) and band shapes as shoulder (sh), sharp (s) and broad (br). UV-Vis absorptions were recorded at 25 °C in the 190-700 nm spectral regions with a Perkin-Elmer Lambda 15 spectrophotometer on NMP solutions by using cell path lengths of 1 cm. ¹HNMR spectra were recorded on a Bruker 300 MHz instrument (Germany). Inherent viscosity was measured by a standard procedure using a Technico[®] viscometer. Thermal Gravimetric Analysis (TGA) data were taken on a Mettler TA4000 System under N₂ atmosphere at a rate of 10 °C/min. The morphology of nanocomposite film was investigated on Cambridge S260 scanning electron microscope (SEM). Elemental analyses were performed by Vario EL equipment.

Table 3. Organic modifiers and Interlayer Distance of the clays.

Type of clay	Organic modifier	Concentration of organic modifier [meq/100 g clay]	Interlayer distance g/cc
Cloisite® 20A		95	1.77

Monomer Synthesis

Synthesis of *N*-trimellitylimido-*L*-Alanine. The diacid **3** was synthesized according to previous work [26].

Polymer Synthesis

In a 100 mL round bottomed flask were placed a mixture of *N*-trimellitylimido-*L*-alanine **3** (0.002 mol), 4,4'-diamino diphenyl ether **4** (0.002 mol), 0.60 g of calcium chloride, 1.2 mL of triphenyl phosphite, 1.0 mL of pyridine and 3.0 mL NMP. The mixture was heated for 1 h at 60 °C, 2 h at 90 °C and then refluxed at 130 °C for 8 h until a viscous solution was formed. Then it was cooled to room temperature and 40 mL of methanol was added to reaction mixture. The precipitate was formed, filtered off and washed with methanol. The resulting polymers **5** were dried under vacuum to leave 0.13 g (97%) of solid polymer. The inherent viscosity of this soluble PAI **5** was 0.64 dL/g. IR (KBr): 3414 (m, br), 3050 (m), 2900 (m), 1780 (m), 1715 (s, br), 1660 (s, br), 1600 (m), 1530 (s), 1500 (s), 1410 (m), 1380 (s), 1320 (m), 1220 (s, br), 1160 (m), 1100 (m), 1090 (m), 1010 (m), 950 (m), 890 (m), 860 (m), 830 (m), 760 (w), 727 (m), 500 (m, br) cm⁻¹. Calcd. for C₂₄H₁₇N₃O₅ (427): C, 67.0; H, 3.6; N, 9.5. Found: C, 67.4; H, 3.9; N, 9.8.

PAI-Nanocomposite synthesis 5a-5d

PAI-nanocomposites **5a-5d** were produced by solution intercalation method, in four different amounts of organoclay particles (5-20 wt.%; increasing in 5 wt.% each) were mixed with appropriate amounts of PAI solution in *N*-methyl-2-pyrrolidone (NMP) to yield particular nanocomposite concentrations. To control the dispersibility of organoclay in poly(amide-imide) matrix, constant stirring was applied at 25 °C for 24 h. Nanocomposite films were cast by pouring the solutions for each concentration into Petri dishes placed on a leveled surface followed by the evaporation of solvent at 70 °C for 12 h. Films were dried at 80 °C under vacuum to a constant weight. Scheme **1** show the flowsheet diagram and synthetic scheme for PAI-nanocomposite films **5a**, **5b**, **5c**, and **5d**.

The water absorption analysis

The water absorption of PAI-nanocomposite films was carried out using a procedure under ASTM D570-81 [27]. The films were dried in a vacuum oven at 80 °C to a constant weight and

then weighed to get the initial weight (W_0). The dried films were immersed in deionized water at 25 °C. After 24 h, the films were removed from water and then they were quickly placed between sheets of filter paper to remove the excess water and films were weighed immediately. The films were again soaked in water. After another 24 h soaking period, the films were taken out, dried and weighed for any weight gain. This process was repeated again and again till the films almost attained the constant weight. The total soaking time was 168 h and the samples were weighed at regular 24 h time intervals to get the final weight (W_f). The percent increase in weight of the samples was calculated by using the formula $(W_f - W_0)/W_0$.

References

- Giannelis, E. P. *Adv. Mater.* **1996**, *8*, 29-35.
- Yano, Y.; Usuki, A.; Kurauchi, T.; Kamigato, O. *J. Polym. Sci. Part A: Polym. Chem.* **1993**, *31*, 2493-2498.
- Zulfiqar, S.; Ahmad, Z.; Ishaq, M.; Saeed, S.; Sarwar, M. I. *J. Mater. Sci.* **2007**, *42*, 93-100.
- Sikka, M.; Cerini, L. N.; Ghosh, S. S.; Winey, K. I. *J. Polym. Sci. Part B: Polym. Phys.* **1996**, *34*, 1443-1449.
- Xu, R.; Manias, E.; Snyder, A. J.; Runt, J. *Macromolecules* **2001**, *34*, 337-339.
- Kausar, A.; Zulfiqar, S.; Shabbir, S. E.; Ishaq, M.; Sarwar, M. I. *Polym. Bull.* **2007**, *59*, 457-468.
- Bibi, N.; Sarwar, M. I.; Ishaq, M.; Ahmad, Z. *Polym. Compos.* **2007**, *15*, 313-319.
- Zulfiqar, S.; Sarwar, M. I. *Scr. Mater.* **2008**, *59*, 436-439.
- Fornes, T. D.; Yoon, P. J.; Hunter, D. L.; Keskkula, H.; Paul, D. R. *Polymer* **2002**, *43*, 5915-5933.
- Chen, G. M.; Ma, Y. M.; Qi, Z. N. *J. Appl. Polym. Sci.* **2000**, *77*, 2201-2205.
- Yano, Y.; Usuki, A.; Kurauchi, T.; Kamigato, O. *J. Polym. Sci. Part A: Polym. Chem.* **1993**, *31*, 2493-2498.
- Ghosh, M. K.; Mittal, K. L. *Polyimides: Fundamentals and Applications*; Marcel Dekker, New York, **1996**.
- Liaw, D. J.; Liaw, B. Y. *Polymer* **2001**, *42*, 839-845.
- Zhang, Q.; Li, S.; Li, W.; Zhang, S. *Polymer* **2007**, *48*, 6246-6253.
- Zhang, Q.; Chen, G.; Zhang, S. *Polymer* **2007**, *48*, 2250-2256.
- Saxena, A.; Rao, V. L.; Prabhakaran, P.V.; Ninan, K. N. *Eur. Polym. J.* **2003**, *39*, 401-405.
- Yang, C. P.; Chen, Y. P.; Woo, E. M. *Polymer* **2004**, *45*, 5279-5293.
- Liaw, D. J.; Chen, W. H. *Polym. Degrad. Stab.* **2006**, *91*, 1731-1739.
- Mallakpour, S.; Kolahdoozan, M. *J. Appl. Polym. Sci.* **2007**, *104*, 1279-1284.
- Faghihi, Kh.; Hajibeygi, M.; Shabani, M. *Macromol. Res.* **2009**, *17*, 739-745.
- Faghihi, Kh.; Shabani, M.; Hajibeygi, M. *Macromol. Res.* **2009**, *17*, 912-918.
- Faghihi, Kh.; Shabani, M.; Izadkhah, A. *Chin. J. Polym. Sci.* **2010**, *28*, 589-596.
- Krishnan, P. S. G.; Wisanto, A. E.; Osiyemi, S.; Ling, C. *Polym. Inter.* **2007**, *56*, 787-795.
- Bharadwaj, R. K. *Macromolecules* **2001**, *34*, 9189-9192.
- Hsiao, S. H.; Yang, C. P.; Wu, F. Y. *Macromol. Chem. Phys.* **1994**, *195*, 2531-2545.
- Zulfiqar, S.; Sarwar, M. I. *J. Incl. Phenom. Macrocy. Chem.* **2008**, *62*, 353-361.